Pressure Drag Measurements for Turbulent Air Flow Through a Packed Bed

D. F. VAN DER MERWE and W. H. GAUVIN

McGill University and Pulp and Paper Research Institute of Canada, Montreal, Canada

Pressure drag coefficients of spheres in a cubic packing of equal spheres have been determined at Reynolds numbers of 27,000, 10,000, 5,000 and 2,500, where N_{Re} is based on superficial air velocity and a sphere diameter of 7 cm. Two cubic arrangements were used: in the regular arrangement, the mean flow was parallel to one of the principal axes, while in the skewed arrangement, the mean flow made equal angles with the three principal axes of the packing.

The pressure drag coefficient of the central sphere has been measured for each of the 12 banks in the regular arrangement, and the effect of bed length has been determined for lengths varying between 1 and 12 banks. The pressure drag coefficient for the central sphere and the overall pressure drop in the skewed arrangement were found to be lower than for the regular arrangement at the same Reynolds number. From the distribution of local pressure measurements, the separation and reattachment points on the central sphere in each bank were determined, indicating that the boundary-layer behavior on a sphere in a packing is similar to that over a single sphere, when allowing for the effects of turbulence and of pressure gradient.

A survey of existing correlations for pressure drop in flow through porous media (*1* to *3*) shows that the flow resistance may be expressed through a friction factor

$$C_f = (\Delta p/L)\,(2d_c/\rho v_c^2) \tag{1}$$

and Reynolds number

$$N_{Re} = v_c d_c/\nu \tag{2}$$

From dimensional considerations, one finds that

$$C_f \sim N_{Re}^{-1} \text{ for low flow rates}$$
$$C_f \sim \text{constant for high flow rates} \tag{3}$$

A much used (*4* to *6*) and recommended (*7*, *8*) interpolation formula has the general form

$$C_f = aN_{Re}^{-1} + b \tag{4}$$

Koida's work (*5*) has shown that the usual assumptions regarding the effects of shape, voidage, and hydraulic radius for porous media lead to different values of b for different types of particles. Koida's work is based on the actual void geometry of the packing. Usually the shape of individual particles and the voidage and specific surface area of the packing are assumed sufficient to characterize the geometry of the packing. Zenz and Othmer (*3*) have discussed the success of various correlations, but have reached the same conclusion as Koida, in general.

Another form of the correlation favored by Carman (*2*), Leva (*9*), and Kast (*10*) is

$$C_f = a\,N_{Re}^{-1} + b\,N_{Re}^{-0.1} \tag{5}$$

However, the equation utilizes the tortuosity of the medium, a property that is of dubious value, since no independent determination of the tortuosity can be made.

The experiments of Martin, McCabe, and Monrad (*11*) have shown the effect of orientation on pressure drop. For the same voidage, the pressure drop in laminar and turbulent flow is remarkably different when the orientation is changed, and no way has been found to correlate the turbulent flow characteristics, although the results in the laminar flow range have been correlated. The laminar flow through a random packing of equal spheres becomes turbulent at $N_{Re} = 115$ (*12*).

The studies by Wentz and Thodos (*13*, *14*) of the pressure drag, of Rhodes and Peebles (*15*) of the local mass transfer, of Wadsworth (*16*), and of Denton (*17*) of the local heat transfer are aimed at elucidating local transfer processes in packed and extended beds. The local heat transfer coefficients tend to show a smaller variation over the surface as the Reynolds number is increased, according to Wadsworth and Denton. Apart from Rhodes and Peebles' interpretation of the relative maxima and minima in the mass transfer coefficient in terms of standing eddies for the cubic packing, the flow in other arrangements is regarded as too complex for analysis.

Rowe and Henwood (*18*) have measured the average drag coefficients in a cubical packing with depth varying between one and eight layers. The average drag coefficient shows a continuously changing value for beds up to five layers in depth, after which it shows little variation.

Rowe and Claxton (*19*) have presented a generalized correlation for heat and mass transfer from a sphere in sphere assemblies, including the cubical arrangement. Their experimental arrangement consisted of four layers of spheres, measurements being conducted in the third layer downstream. The experiments used air and water in the third layer downstream. The experiments used air and water in the Reynolds number range $20 < N_{Re} < 2{,}000$. The voidage was the determining parameter in the value assigned to the coefficients A and B, while the exponent n was a function of N_{Re} in their correlation for heat transfer:

$$N_{Nu} = A + B(N_{Pr})^{1/3}(N_{Re})^n \tag{6}$$

Wentz and Thodos' (*13*, *14*) pressure drag determinations were made on the central sphere in the middle layer of a bed consisting of five layers. A comparison of their results with those of Rowe and Henwood (*18*) points out the need for detailed knowledge of flow development in a packed bed, since the value of the measured pressure drag coefficient may not be representative of the average pressure drag coefficient in a larger bed. Malling and Thodos (*20*) eliminated entry and exit effects by adding three inert layers to the upstream and downstream ends

D. F. van der Merwe is at the University of Witwatersrand, Johannesburg, South Africa. W. H. Gauvin is at Noranda Research Centre, Pointe Claire, Quebec, Canada.

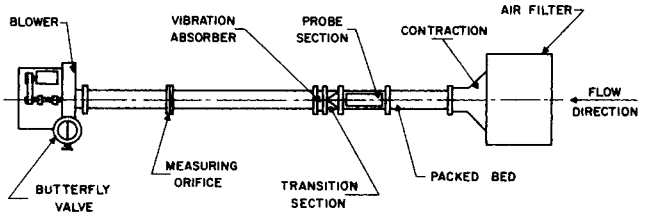

Fig. 1. Schematic drawing of experimental arrangement.

of the packing used in determining the average heat and mass transfer coefficients. Their results are applicable to long beds where entry and exit effects may be ignored. In laboratory studies short beds are often employed to reduce the effects of axial mixing (*21*).

One concludes first that before the analogy between skin friction and heat transfer recently proposed for packed beds by Tallmadge (*22*) can be accepted, more detailed information regarding flow development is required. A study of flow development would also serve to place the work of other investigators in a better perspective. Second, one concludes that the effect of void geometry on flow resistance is uncertain in the turbulent flow regime.

EXPERIMENT

Since theoretical calculations of the turbulent shear flow through a porous medium was out of the question, a simple experimental investigation was planned to determine the effect of void geometry on resistance, and to study the detailed flow behavior over the whole length of a packed bed. Only the drag coefficient measurements are reported here. Results on the mean velocity and turbulence characteristics of the flow in the pores will be published separately.

Two identical cubic packings of equal spheres were accordingly selected, but in different orientations, to allow a comparison of the effect of the void orientation under constant packing geometry.

Apparatus

Figure 1 shows schematically the experimental arrangement, which consisted of an air filter, a contraction (11-in. deep, 330-in. radius, 90 deg. plywood wedge, with a copper wire screen and a honeycomb at the entrance of the wedge) which was faired smoothly to the 11-in. square cross section of the model packed bed. The latter was followed by a Lucite duct with an air-tight removable lid to allow access to probes installed to the rear of the bed. This section also provided sufficient length for pressure recovery in pressure measurements across the bed. Following a transition section and a 6-in. wide vibration absorber, the volumetric rate of flow was measured in a 10-in. I.D. aluminum duct, 12¼-ft. long, with a 7¾-ft. long calming section ahead of a 4-in. diam. sharp-edged orifice with radius taps. For the two lower flow rates, a 4-in. I.D. duct, 9¼-ft. long, was used, with a 6¼-ft. long calming section leading to a 0.8-in. diam. orifice with radius taps. A Westinghouse centrifugal compressor, Model 25061, 15-hp., 10,000 cu.ft./min., 30-in. water gauge at 200°F. and 3,500 r.p.m., supplied the draught, while a butterfly valve at the fan exhaust controlled the volume flow. Both model packed beds used a cubical packing of equal 70-mm. diam. spheres, spun from aluminum and supported on 0.375-in. diam. aluminum tubing in air-tight Lucite frames.

The regular arrangement consisted of 10 banks of spheres, a single bank being formed by nine full spheres with half and quarter spheres to fill in the sides of a 28-cm. square Lucite frame. The mean flow direction was parallel to one of the principal axes of the packing. To describe the probe location in the bed, two right-handed rectangular coordinate systems were used, as shown in Figure 2. The porosity of a cubic packing, defined as the ratio of the void volume to the total volume, is 0.476.

Every bank had a static pressure tap 1 in. behind the center line of the spheres in the bank. Additional pressure taps were provided at the same spacing in the contraction ahead of the bed, and in the square duct behind the bed, to determine the actual pressure drop across the complete bed after pressure recovery, as well as to give an indication of the pressure drop across individual banks in the bed.

The skewed arrangement derived its name from the fact that the spheres, although in a cubical packing and filling again an 11-in. (28-cm.) square Lucite duct, were arranged on 0.375-in. diam. rods at such an angle that the mean flow direction made equal angles with the three principal axes of the packing. The total length of the bed in the skewed arrangement equalled about 14 sphere diameters. The porosity in the skewed arrangement was, of course, the same as in the regular arrangement.

Instrumentation

Sphere for Pressure Drag Determinations. The pressure drag of a sphere in a packed bed was determined by measuring the distribution of the normal pressure over the surface of a special sphere equipped with equally spaced 0.007-in. diam. pressure taps connected to 0.0625-in. diam. tubes which passed through the 0.375-in. diam. supporting tube. This sphere could be inserted in any desired location in any bank of spheres.

The spacing of the taps could be specified in a spherical coordinate system (r, ϕ, θ) with origin at the center of the sphere, as shown in Figure 2. The 11 taps were located at θ = 15, 30, 45, 60, 75, 90, 105, 120, 135, 150, 165 deg., 5 taps in one part and 6 taps in the other part of the sphere which was cut in two beyond the θ = 90 deg. plane. A graduated scale mounted on the supporting tube indicates the angle ϕ through which the sphere was rotated. It is to be noted that the pressure measurements were made around the complete sphere and on a finer grid than previously used (*14*) and are therefore believed to be more accurate.

Pressure measurements. Some of the pressure readings were obtained with a multitube manometer with methanol as the indicating fluid, and at an inclination of 25 deg. to the horizontal. The bulk of the pressure readings was recorded with a Statham pressure transducer, 0.1 lb./sq.in. rating, in conjunction with an automatic scanning device and a strip chart recorder available as a self-contained unit.

Procedure

The experiments were carried out at the following four nominal superficial velocities (U_0) and Reynolds numbers:

Superficial velocity, cm./sec.	Reynolds number
605	27,000
225	10,000
112	5,000
56	2,500

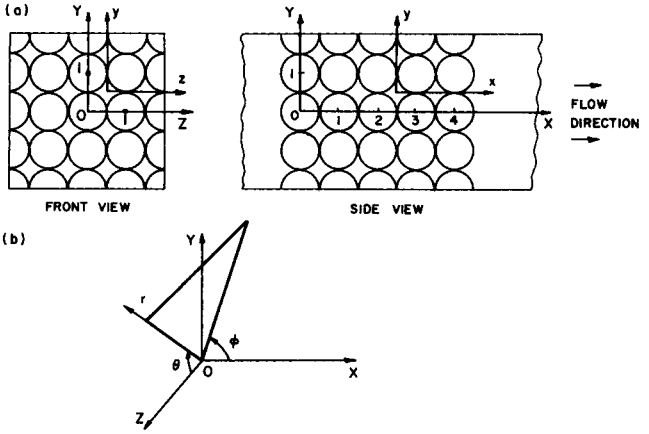

Fig. 2. Coordinate systems used in packed bed. *(a)* Rectangular coordinate systems: *(X,Y,Z)* specify location in bed; *(x,y,z)* specify location in pore. *(b)* Spherical coordinate system.

The approach velocity was uniform over the duct entrance area up to the boundary layer at the wall, which was about 5 mm. thick at the highest Reynolds number. The turbulence level was less than 1%.

For a given run, the orifice manometer reading was checked about 20 min. after the blower had been turned on and adjusted to the correct value, whereupon it remained constant for several hours, barring any rapid change in atmospheric temperature and pressure. The readings of the normal pressure on the sphere were then taken at 5 deg. intervals of ϕ for the 11 pressure taps. The pressure drop across the bed was read at the same time on a single inclined tube manometer. In the case of the pressure transducer, a 4-sec. interval was deemed adequate to register the average pressure. On the multitube manometer, it was observed that the pressure distribution showed a slight irregular oscillation between two states, it being impossible to say which was the more stable state. This oscillation was much more serious in the case of a single bank of spheres.

Presentation of Pressure Distribution. The normal pressure recorded on the surface of the sphere was below atmospheric pressure, which was also the reference pressure. A pressure coefficient C_p was defined as

$$C_p = 2p/\rho U_0^2 \tag{7}$$

The pressure determinations were specified with respect to the angles ϕ and θ of Figure 2.

Pressure Drag Coefficients. Numerical integration of the x component of the normal pressure on the sphere gives the total force in the x direction, and thus the pressure drag coefficient

$$C_{Dp} = (2/\pi\rho U_0^2) \int_0^{\pi} \int_0^{2\pi} p(\phi, \theta) \cos\phi \sin^2\theta d\phi d\theta \tag{8}$$

EXPERIMENTAL RESULTS

Measurements on Single Spheres in Line and Single Banks of Spheres

Values of the pressure drag coefficient C_{Dp} at $N_{Re} =$ 27,000 on a single sphere, two spheres in line, and three spheres in line (the flow being parallel to the line connecting the spheres) are presented in Table 1. Also included in this table are the pressure drag coefficients for the central sphere in a single bank of spheres ($N_{Re} =$ 27,000 and $N_{Re} =$ 10,000) located in the wake of a single bank of spheres, five sphere diameters upstream. It should be pointed out that the values of the Reynolds number for single spheres and for packed beds are both based on the same characteristic dimensions, namely, the sphere diameter and the superficial or approach velocity just ahead of the sphere or of the packing. The two values of N_{Re} are not directly comparable, however, since the actual velocity in the pores of the packing is, in effect, very much higher. A detailed study of the velocity profiles in the pores of the packing will be presented in a subsequent paper.

Effect of Bed Length on Drag Coefficient

At a nominal Reynolds number of 27,000, the pressure drag coefficient of the central sphere in a bank of the regular arrangement was determined for all sphere positions from the upstream to the downstream end of the bed, the number of banks being varied from 1 to 12. These pressure drag coefficients are presented in Table 2.

Variation of Pressure Drag Coefficient with Reynolds Number

For the regular arrangement with 10 banks, the pressure drag coefficient of the central sphere in all banks was determined for $N_{Re} =$ 27,000 and $N_{Re} =$ 10,000. They are shown in Figure 4. The pressure drag coefficients for the first four banks of the regular arrangement were determined for $N_{Re} =$ 5,100 and $N_{Re} =$ 2,500. The values were 24.9, 3.0, 7.6, and 6.8, respectively, for $N_{Re} =$ 5,100 and 21.6, 3.9, 8.0, and 6.8, respectively, for $N_{Re} =$ 2,500. Finally, the pressure drag for the central sphere in the skewed arrangement was also determined at the two higher Reynolds numbers; the values will be discussed later.

DISCUSSION

Accuracy of Measurements

The individual pressure readings on the multitube manometer and the strip chart recorder, associated with the pressure transducer, could be read with a precision of 0.1%. The uncertainty in the density of the manometer fluid and the pressure transducer calibration was of the same order of magnitude. The greatest uncertainty arose on account of pressure fluctuations mentioned earlier, associated with variations in the position of the separation lines on the spheres. Severe oscillations between two states appear to exist for flow behind a single bank. The relatively mild oscillations that occur in all wake-like regions reduced the precision to about 0.5%; the precision for severe oscillations was 2.5%. Thus the uncertainties in the pressure drag coefficient were 3% on the average and 11% in the case of a single bank (allowance being made for the precision in measuring the angle ϕ). In this respect, the measurements with the automatically scanning pressure transducer present a time-averaged pressure drag coefficient, provided the fluctuations occur randomly.

Measurements on Single Spheres, Spheres in Line, and Single Banks of Spheres

The fact that the measured pressure drag coefficient $C_{Dp} = 0.44$ for a single sphere (Table 1) is very close to the standard value for the total drag coefficient C_D is regarded as probably coincidental, rather than as a confirmation of experimental accuracy, since the support of the sphere and the effects of blockage should cause a small error in the measurements.

With the flow parallel to two spheres in line (see Table 1), the pressure drag of the combination is less than the pressure drag of a single sphere, the pressure drag of the upstream sphere being reduced, in qualitative agreement with the experiments of Rowe and Henwood (*18*) on chains of spheres (involving the total drag). The negative pressure drag obtained on the second downstream sphere

TABLE 1. PRESSURE DRAG COEFFICIENTS ($N_{Re} = 27{,}000$)

A. Drag Coefficient of a Single Sphere

Single sphere		
Drag coefficient:	0.44	
Reynolds number:	27,300	
Two single spheres in line		
	First sphere	Second sphere
Drag coefficient:	0.41	−0.02
Reynolds number:	26,400	26,700
Three single spheres in line.: sphere in center		
Drag coefficient:	−0.10	
Reynolds number:	26,200	

B. Single Bank of Spheres

In unperturbed stream		
Drag coefficient:	15.95	18.36
Reynolds number:	26,800	9,840
In wake of single bank five sphere diameters upstream		
Drag coefficient:	16.05	19.44
Reynolds number:	26,400	9,840

for two or three spheres in line is in qualitative agreement with results for cylinders presented by Hoerner (23).

The Reynolds number of 27,000 is far below the critical Reynolds number for the low turbulence air stream (24). The lower drag of the upstream sphere, for two spheres in line, is probably due to the stabilizing effect exerted by the downstream sphere on the wake of the upstream sphere. The separated laminar boundary layer of the upstream sphere can be expected to reattach as a turbulent boundary layer on the downstream sphere. But although a laminar separation is indicated by the pressure distribution around the first sphere, the characteristic delayed separation associated with a turbulent boundary layer is not apparent on the second sphere, except that separation apparently takes place at $\psi > 90$ deg., where ψ is the angle from the forward stagnation point ($\psi = \pi - \phi$). The limited accuracy of the measurements and the amount of experimental data do not permit one to draw any further conclusions, or to compare the measurements for three spheres in line.

Rowe and Henwood (18) did not find a Reynolds number dependence in their experiments on a single bank of spheres. That one should exist, as was found in the present study (see Table 1), can be expected. At the higher Reynolds number, the acceleration of the boundary layer due to the favorable pressure gradient on the forward part of a sphere in a bank is likely to delay separation until ψ is equal or larger than 90 deg., except near the points of contact; whereas at the lower N_{Re}, separation will take place farther upstream. This is the case for closely spaced cylinders (25).

The effect of the turbulence generated by a single bank of spheres, five sphere diameters upstream, on the pressure drag of a sphere in a single bank produced slightly higher values of C_{Dp}, but the variation was within the experimental error. No turbulence measurements have been made, but judging from the turbulence generated by grids (26), one expects the turbulence level to be of the order of 8%. It appears that the turbulence level was insufficient to overcome the effects of a contracting stream and an accelerating boundary layer, and to cause a transition to turbulence in the boundary layer over the upstream half of the sphere, as was shown to occur at higher turbulence intensities by Torobin and Gauvin (24). However, from the greater scatter in the pressure readings over the the downstream half of the sphere, it appears that the turbulence did promote an earlier transition in the separated layer at times, causing the subsequent reattachment line to move irregularly.

Variation of Pressure Drag Coefficient with Position and Bed Length

The results giving the variation of C_{Dp} with position and bed length are presented in Table 2. The experiments have all been performed at a Reynolds number of 27,000 on the central sphere of a bank in the regular arrangement, the number of banks varying between 1 and 12.

Two drag ratios may be formed to compare these results to the work of Rowe and Henwood (18). Let $\overline{C_D}$ denote the average drag coefficient of a sphere in the assembly as determined from the overall pressure drop, as in Equation (1). The average pressure drag coefficient $\overline{C_{Dp}}$ is the average of the pressure drag coefficients C_{Dp} for the central spheres of the banks forming the bed. The drag coefficient C_D of a single sphere at the same Reynolds number is used to form the drag ratios $\overline{C_D}/C_D$ and $\overline{C_{Dp}}/C_D$. This value of C_D was 0.44. Figure 3 shows the drag ratios obtained here in comparison to the drag ratios of Rowe and Henwood (which included pressure as well as viscous drag).

The drag ratio $\overline{C_{Dp}}/C_D$ for a single bank of spheres at $N_{Re} = 27{,}000$ is 35.5, as compared to 36.7 in Rowe and Henwood's experiments at $N_{Re} = 300$. For two banks, Rowe and Henwood actually found an increase in average drag, and, if correct, this is probably another indication of the different behavior of the boundary layer at $N_{Re} = 27{,}000$. For the Reynolds number of 300, at which Rowe and Henwood have performed their experiments, separation is expected to occur at values of $\psi \geqq 90$ deg. for the sphere in the upstream bank, except near points of contact. With the addition of a second bank downstream, the separated flow will attach to the downstream sphere, but separation is not expected to occur beyond $\psi = 90$ deg., as is the case for the upstream bank. The attaching flow is not only perturbed by the variations that occur in the recirculating flow between the spheres, but the pressure gradient over the downstream spheres is not as strongly favorable as during the initial contraction of the stream passing through the first bank. The wake behind the second sphere is therefore expected to be larger than for a sphere in a single bank, with a corresponding increase in the pressure drag, as observed by Rowe and Henwood. At the higher Reynolds number of 27,000 used in this study, on the other hand, and as shall be shown later from a detailed study of the pressure distributions, the boundary layer on the sphere in the downstream bank is expected to be turbulent (24). The turbulent boundary layer will separate at $\psi > 90$ deg. on the downstream bank, and will give a reduced pressure drag on account of the smaller wake size. As a matter of

TABLE 2. VARIATION OF PRESSURE DRAG COEFFICIENT IN PACKED BED FOR DIFFERENT LENGTHS OF THE REGULAR ARRANGEMENT ($N_{Re} = 27{,}000$)

No. of banks	0,0,0	1,0,0	2,0,0	3,0,0	4,0,0	5,0,0	6,0,0	7,0,0	8,0,0	9,0,0	10,0,0	11,0,0
12	14.9	2.1	5.4	6.0	7.2	7.1	6.9	7.0	7.3	7.1	6.4	6.7
11	14.4	2.4	5.4	6.2	7.0	7.2	6.9	6.8	7.4	8.0	7.1	6.7
10	14.3	2.4	5.4	6.4	6.9	6.9	7.1	7.2	7.7	6.8		
9	14.2	2.0	5.3	6.8	6.5	6.8	7.0	7.2	5.7			
8	14.5	1.9	4.9	7.0	6.9	7.4	7.5	6.8				
7	14.8	2.4	5.8	6.4	7.2	7.3	6.9					
6	15.0	2.6	5.7	5.9	6.7	6.2						
5	14.7	2.4	5.3	6.1	6.2							
4	14.8	2.4	5.6	5.8								
3	15.3	2.3	5.5									
2	15.5	3.1										
1	15.6											

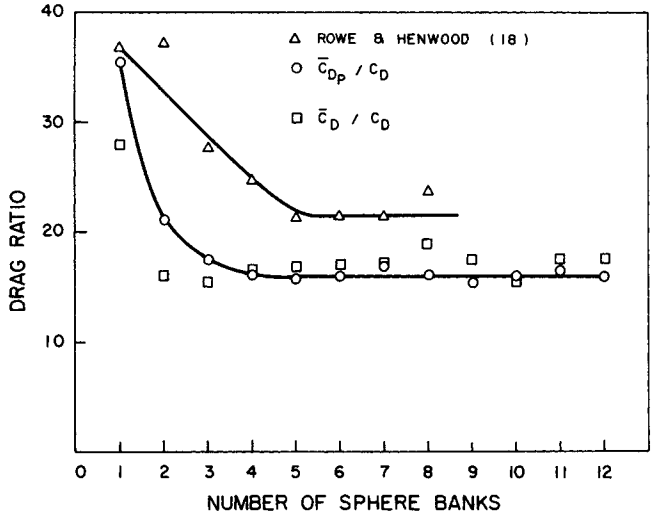

Fig. 3. Drag ratios $\overline{C_D}/C_D$ and $\overline{C_{Dp}}/C_D$ for regular arrangements of various lengths compared to drag ratios obtained by Rowe and Henwood (18).

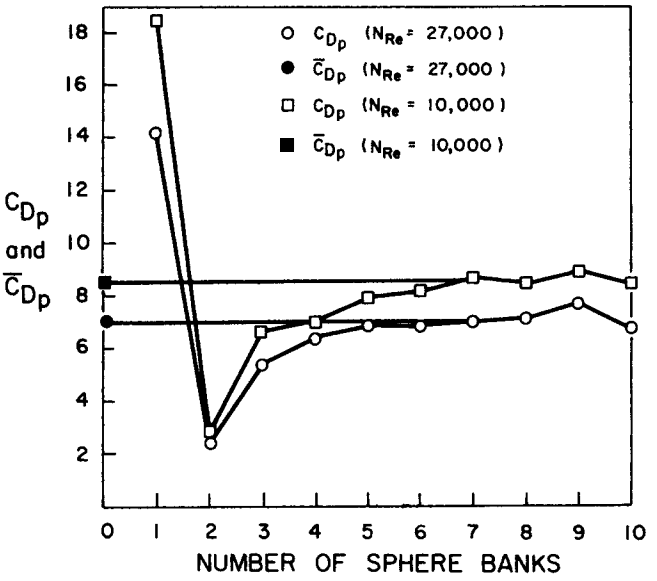

Fig. 4. Comparison of C_{Dp} for a regular arrangement of 10 banks at Reynolds numbers of 27,000 and 10,000.

fact, the pressure drag on the downstream sphere might be expected to be negative, as in the case for two spheres in line parallel to the oncoming stream (see Table 1), since the boundary-layer behavior should be qualitatively similar when allowing for the effects of the pressure gradient. In reality, the pressure drag on the sphere in the downstream bank is not negative, but is six times lower than on the sphere in the first upstream bank of the bed. The drag is not negative on account of the pressure gradient in which the two banks of spheres find themselves; this pressure gradient results from the contraction of the stream to pass through the void space between the spheres and the energy loss following the stream expansion behind the downstream bank. This gradient is hardly perceptible for two spheres in line in a uniform stream. The effect of putting spheres in a bank tends to fix the separation line on the sphere; readings on the multitube manometer are reported to have steadied when adding a second bank.

It appears that the limiting value of 16 for the drag ratio $\overline{C_{Dp}}/C_D$ is reached at $N_{Re} = 27{,}000$ with four banks of spheres. This limiting ratio is smaller than the value of 21.3 found by Rowe and Henwood at $N_{Re} = 300$, after five banks of spheres. But since the latter value is based on pressure as well as viscous drag, and viscous drag is still appreciable at $N_{Re} = 300$, the trends are according to expectations for the limiting values of the drag ratios and the number of banks required to reach the limiting value.

Despite the large scatter in the drag ratio $\overline{C_D}/C_D$ at $N_{Re} = 27{,}000$, the limiting value of this drag ratio appears to be slightly larger than that of $\overline{C_{Dp}}/C_D$, although smaller initially. The lower initial values are attributed to the wall's interfering effect on the development of the wake regions behind the spheres near the wall, causing them to have lower drag values and thus lowering the average values for the first two banks. Once turbulent flow is established, however, the presence of the wall will lead to relatively greater energy losses compared to the flow further away from the walls. This line of reasoning presupposes that apart from greater dissipation close to the walls, the mean flow is everywhere much the same, that is, no wall effect is present. Mickley, Smith, and Korchak (27) have used a rhombohedral packing of equal spheres, and have utilized sphere sections to preserve uniformity of the packing up to the wall, but found that a peak in the velocity profile occurred 1.5 sphere diameters away from the wall. However, uniformity of the packing arrangement near the wall is not sufficient to ensure uniformity of the flow. Uniformity of the flow is achieved only when the symmetry of the packing does not impose physically unrealistic flow behavior, as is the case with the blocked void passages of a rhombohedral packing near the wall. No wall effect is expected in the case of a regular cubic packing and other measurements have confirmed the absence of a wall effect for mean velocity distribution in the regular arrangement (28).

It is not warranted to conclude from the plot of the drag ratio $\overline{C_{Dp}}/C_D$ on Figure 3 that four or five banks are sufficient to establish a bed which would be representative of a long bed. Comparison of the individual pressure drag coefficients of Table 2 with the corresponding values of $\overline{C_{Dp}}$ in Figure 4 clearly shows that only with seven or eight banks does one find banks in the interior of the bed with a pressure drag coefficient C_{Dp} equal to the average pressure drag coefficient of the bed as a whole. This should caution one to regard the measurements of Wentz and Thodos (14) as representative of a cubic packing. The same reservation applies to the subsequent effort of Tallmadge (22), which is based on their results.

Effect of Reynolds Number and Orientation on the Pressure Drag Coefficient

Comparison of the values of C_{Dp} given earlier at nominal Reynolds numbers of 10,000 and 27,000 shows that the flow development is very similar, apart from the consistently higher pressure drag coefficient obtained for $N_{Re} = 10{,}000$, as better shown in Figure 4. The measurements at the nominal Reynolds numbers of 5,000 and 2,500 are limited but are sufficient to show a similar trend in the sharp drop in pressure drag coefficient for the second sphere, but differ in that the pressure drag coefficient for the third bank shows a relative maximum. Furthermore, the pressure drag coefficient for the first bank at $N_{Re} = 2{,}500$ is lower than the pressure drag coefficient at $N_{Re} = 5{,}000$, which is contrary to the trend of increasing pressure drag coefficient with lower Reynolds numbers observed at the other Reynolds numbers. Also, the decrease in pressure drag for the second bank is less than at the higher Reynolds numbers.

The measurements of Wentz and Thodos (14) on a cubic packing have been made in a lower Reynolds num-

ber range, namely, $1,540 \leqq N_{Re} \leqq 6,920$. The pressure drag coefficients that one may calculate from their data are higher by 29 and 19% than the present values found in a packed bed of double their length, but at the same distance downstream in the bed. Readings taken at $N_{Re} = 2,500$ indicate the presence of severe pressure oscillations, and the rather different trend observed at the lowest Reynolds number may be partly due to experimental inaccuracy. However, the data of Wentz and Thodos do not show a monotonic increase in the pressure drag coefficient for Reynolds numbers below 6,000.

The pressure drag determinations in the skewed arrangement have been made on a centrally located sphere in the middle of the bed, about seven sphere diameters from the upstream end of the bed. At Reynolds numbers of 27,000 and 10,000 the values of C_{Dp} were 5.9 and 7.9, respectively. These values are about 17 and 8% less than the average pressure drag for a sphere (7.1 and 8.6; see Figure 4) in the regular arrangement at the corresponding Reynolds numbers. The measurements of the overall pressure drop show a similar trend which is certainly contrary to expectations. The differences are well above the limit of experimental accuracy, and an explanation requires a detailed examination of the flow and pressure distribution in the skewed arrangement, as given in the following section.

Pressure Distribution over Spheres

The comments that have been made on the variation of the pressure drag coefficients, as determined by the boundary-layer behavior, will now be supported by a closer examination of the measured pressure distributions. Table 3* summarizes the results of local pressure measurements at Reynolds numbers of 27,000 and 10,000 through a regular arrangement of 10 banks of spheres at $\theta = 45$ and 60 deg. Data at 135 and 150 deg. were almost identical with those at 45 and 60 deg., respectively, indicating good symmetry in the experimental arrangement. In interpreting these results, it must be remembered that the pressures recorded are below atmospheric pressure, hence the lowest figures correspond to the highest absolute pressures.

The pressure distribution for the upstream bank, Run 102, shows for the angles $\theta = 60$ deg. and $\theta = 45$ deg. a rather similar behavior, which is more akin to the flow over a cylinder than the flow over a single sphere. The flow separates at $\psi = 90$ deg., the pressure showing a slight dip before taking on an almost constant value in the wake region. The latter has a pressure that is considerably lower than the pressure on the upstream part of the sphere (bearing in mind that the figures shown are below atmospheric).

On the second sphere (Run 104), the jet formed in the narrowest cross section of the upstream bank with separation of the flow attaches at $\psi \cong 35$ deg. for $\theta = 60$ deg. and at $\psi \cong 30$ deg. for $\theta = 45$ deg. These estimates are based on the assumption that the pressure rises at reattachment. The pressure distributions for $\theta = 60$ deg. and $\theta = 45$ deg. show a behavior resembling that of a turbulent boundary layer, in that there is a pressure recovery or rise after $\psi = 90$ deg., the wake region commencing at about $\psi = 130$ deg. Since the expansion of the flow after passing through the constriction offered by the second bank is considerable, the pressure differences over the upstream and downstream sides of the second bank are not very large. Without further experimental evidence it is idle to speculate whether the attaching shear layer is laminar; shear layers behind cylinders are laminar for very low values of the Reynolds number only (*30*).

The pressure distribution for the spheres in the fourth (Run 108) and fifth banks (Run 110) are quite similar, showing that the flow reattaches at $\psi = 40$ deg. and separates at ψ about 135 deg. A comparison with the pressure distribution over a sphere in the seventh bank (Run 114) shows quite similar behavior to the flow over the fifth bank, the flow reattaching and separating at the same values of ψ, but with a larger pressure difference between the upstream and downstream parts of the sphere.

One should keep in mind that the points of reattachment and separation are difficult to estimate precisely from the pressure distribution. Also, irregular changes in the points of separation and reattachment occur, so that the values of ψ quoted above may vary from one experiment to another. Variations of a few degrees in the location of separation and reattachment points cannot necessarily be ascribed to differences in flow behavior.

For the central spheres in the first, fifth, and seventh banks in the regular arrangement at a Reynolds number of 10,000 (Runs 103, 111, and 115) the flow pattern appears to be similar with regard to the positions of reattachment and separation.

The limited amount of information obtained at the two lower Reynolds numbers makes it difficult to comment. In addition, the measurements made at a Reynolds number of 2,500 show a large amount of scatter. However, the behavior of the pressure distribution appears to be similar to that at a Reynolds number of 27,000, except that the pressure distribution over the sphere in the second bank does not show the symmetrical shape around $\psi = 90$ deg. occurring at higher Reynolds numbers, and separation takes place at $\psi = 110$ deg. for a Reynolds number of 5,000 and $\psi = 100$ deg. for a Reynolds number of 2,500.

The local mass transfer coefficients on a 1.5-in. diam. sphere in the center of the fifth layer of a square cubic arrangement, five sphere diameters wide, and seven sphere diameters long, have been measured by Rhodes and Peebles (*15*) at Reynolds numbers of 2,409, 1,810, and 488. There appears to be qualitative agreement between their measurements and the present pressure distribution at a Reynolds number of 2,500. The flow entering the arrangement of Rhodes and Peebles probably possesses a higher turbulence level than the flow used for the present pressure drag determinations, but the effect is probably not significant at the fifth downstream layer of the bed, but would be for the third layer in Wentz and Thodos' work.

Data for the pressure distribution of a sphere in the center of a bed in the skewed arrangement at $N_{Re} = 26,460$ (Run 301) are given in Table 4.* The flow over the sphere may be interpreted in the same way as for the regular arrangement, remembering that ψ and θ have their usual significance with respect to the mean flow direction, but that the latter now make equal angles with the three principal axes of the packing. The flow is everywhere blocked and all six apertures to a given packing void contribute to it. It appears that what might be termed the wake region of the surface is smaller than in the case of the regular arrangement. The variation of the pressure

* Table III has been deposited as document 01321 with the ASIS National Auxiliary Publications Service, c/o CCM Information Sciences, Inc., 909 Third Ave., New York 10022 and may be obtained for $2.00 for microfiche or $6.50 for photocopies.

* Table IV has been deposited as document No. 01321 with the ASIS National Auxiliary Publications Service, c/o CCM Information Sciences, Inc., 909 Third Ave., New York 10022, and may be obtained for $2.00 for microfiches or $6.50 for photocopies.

distribution associated with a turbulent boundary layer over the surface of a sphere is not observed to the same extent as in the regular arrangement. In fact, there is a gradual pressure recovery reminiscent of the attached flow of a thin jet around a cylinder (*32*). In the regular arrangement, only two of the six entrances to a given void contribute to the mean flow. Presumably in the skewed arrangement, after passing through one of the six apertures to the void, the flow through two adjoining entrances provides sufficient additional momentum to delay separation until the flow has to pass through the entrance it encounters next. Smaller pressure differences between front and back result, which account for the lower pressure drag coefficient and the lower overall pressure drop of the bed, compared with the regular arrangement.

CONCLUSIONS

With a description of the flow available from the measurement of pressure distributions, the systematic analysis of the resistance of a porous medium in the turbulent regime becomes possible. Generally speaking, it appears that the boundary-layer behavior on a sphere in a packing remains similar to the behavior over a single sphere, when allowing for the effects of turbulence and of pressure gradient. Thus the pressure distributions lead to the following qualitative description of the flow in the regular arrangement: the laminar boundary layer on a sphere in the first bank separates at an angle ψ of close to 90 deg. It reattaches on the second sphere at ψ about 30 deg. The spreading of the jet in the first pore is relatively small, the potential core forming a large part of the jet cross section. In the second pore, the potential core is smaller, the turbulence level is higher, and the jet boundary is more diffuse. The boundary layer on the second and subsequent spheres in the bed is turbulent and separates at ψ about 130 deg. on the second sphere, and somewhat later in the body of the packed bed, with reattachment at ψ about 40 deg. This trend continues in subsequent banks, but with diminishing effect, the pressure distribution for the fifth and sixth layers appearing to be quite similar. Over the final, tenth bank of spheres, the sudden change in the pressure gradient due to the abrupt expansion of the flow, is expected to diminish the measured pressure drag coefficient. This picture is qualitatively in accord with the known experimental results on the effect of turbulence on the drag coefficient of single spheres (*24, 31*).

Finally, the following points should be noted:

1. It appears that a considerably longer cubic packing is required than has been deemed necessary by a number of other investigators to obtain an environment for a sphere that is representative of a large bed. The very large pressure drag of the upstream bank of spheres, compared to those following downstream, gives rise to an uneven weighting of pressure drag coefficients when the overall drag of the assembly is computed, and gives the mistaken impression that five banks of spheres are representative of a large packing.

2. The pressure drag coefficient at the lower Reynolds number of 10,000 behaves in a similar way as at $N_{Re} =$ 27,000, except that fully developed flow conditions are obtained later, according to Figure 4. The measurements at the lower Reynolds numbers of 5,000 and 2,500 were inconclusive due to a limited number of experiments.

3. The skewed arrangement shows a lower pressure drag coefficient than the regular arrangement. The difference in pressure drag between the regular and skewed arrangements decreases as the Reynolds number is reduced from 27,000 to 10,000.

ACKNOWLEDGMENT

Financial assistance from the National Research Council of Canada, the Commonwealth Scholarship and Fellowship Association, and the South African C.S.I.R. is gratefully acknowledged.

NOTATION

a = constant in Equations (4) and (5)
A = constant in Equation (6)
b = constant in Equations (4) and (5)
B = constant in Equation (6)
C_D = (total) drag coefficient of a single sphere
$\overline{C}_D$ = (total) average drag coefficient of a sphere in packed bed
C_{Dp} = pressure drag coefficient for sphere
$\overline{C}_{Dp}$ = average pressure drag coefficient of a sphere in bed
C_f = friction factor as defined by Equation (1)
d = sphere diameter
d_c = characteristic length for packing (equal to the sphere diameter for a packing of uniform spheres)
L = length of packed bed
N_{Nu} = Nusselt number
N_{Pr} = Prandtl number
N_{Re} = Reynolds number, Equation (2)
p = pressure
p_0 = pressure in free stream
r = coordinate in spherical coordinate system (r, ϕ, θ)
U_0 = superficial velocity of flow through bed, equal to the approach velocity just ahead of the packing
v_c = characteristic velocity for packing (taken as U_0, unless otherwise specified)
X, Y, Z = coordinate system defining location in bed
x, y, z = coordinate system defining location in pore
θ = angle in spherical coordinate system (r, ϕ, θ)
ν = kinematic viscosity of fluid
ρ = density of fluid
ϕ = angle in spherical coordinate system (r, ϕ, θ)
ψ = $\pi - \phi$

LITERATURE CITED

1. Scheidegger, A. E., "The Physics of Flow Through Porous Media," Chap. VII, Toronto Univ. Press, Canada (1960).
2. Carman, P. C., "Flow of Gases Through Porous Media," Chap. VII, Academic Press, New York (1956).
3. Zenz, F. A., and D. F. Othmer, "Fluidization and Fluid-Particle Systems," Chap. V, Reinhold, New York (1960).
4. Ergun, S., *Chem. Eng. Progr.*, **48**, 89 (1952).
5. Koida, N. U., *Russian J. Phys. Chem.*, **34**, 375 (1960).
6. Ward, J. C., *J. Hydraulics Div. ASCE*, **90**, HY5-1 (1964).
7. Andersson, K. E., *Trans. Royal Inst. Technol. No. 131* (1963).
8. Collins, R. E., in "Modern Chemical Engineering," A. Acrivos, ed., Vol. 1, p. 323, Reinhold, New York (1963).
9. Leva, M. et al., *U.S. Bur. Mines Bull. No. 504* (1951).
10. Kast, W., *Chem.-Ing.-Tech.*, **36**, 464 (1964).
11. Martin, J. J., W. L. McCabe, and C. C. Monrad, *Chem. Eng. Progr.*, **47**, 91 (1951).
12. Jolls, K. R., Ph.D. dissertation, Univ. Illinois, Urbana (1966).
13. Wentz, C. A., and George Thodos, *AIChE J.*, **9**, 81 (1963).
14. *Ibid.*, 358 (1963).
15. Rhodes, J. M., and F. N. Peebles, *ibid.*, **11**, 481 (1965).
16. Wadsworth, J., *Natl. Res. Council, MT-41* (1960).
17. Denton, W. H., "General Discussion on Heat Transfer," p. 370, Inst. Mech. Eng., London (1951).
18. Rowe, P. N., and G. A. Henwood, *Trans. Inst. Chem. Eng.*, **39**, 43 (1961).
19. Rowe, P. N., and K. T. Claxton, *ibid.*, **43**, T321 (1965).
20. Malling, G. F., and George Thodos, *Intern. J. Heat Mass Transfer*, **10**, 498 (1967).

21. Epstein, Norman, *Can. J. Chem. Eng.*, **36**, 210 (1958).
22. Tallmadge, J. A., *AIChE J.*, **13**, 599 (1967).
23. Hoerner, S. F., "Fluid-Dynamic Drag," 148 Busteel Drive, Midland Park, N. J. (1958).
24. Torobin, D. B., and W. H. Gauvin, *AIChE J.*, **7**, 615 (1961).
25. Roberts, B. W., *J. Royal Aeronaut. Soc.*, **70**, 886 (1966).
26. Forster, H., and G. Apel, *Maschinenbautechnik*, **14**, 193 (1965).
27. Mickley, H.S., K. A. Smith and E. I. Korchak, *Chem. Eng. Sci.*, **20**, 237 (1965).
28. Mujumdar, A., personal communication (1968).
29. D. F. van der Merwe, Ph.D. thesis, McGill Univ., Quebec (1968).
30. Roshko, A., and J. C. Lau, "Proc. 1965 Heat Transfer and Fluid Mechanics Institute," A. F. Charwat et al., eds., p. 158, Stanford Univ. Press, Calif. (1965).
31. Clamen, A., and W. H. Gauvin, *AIChE J.*, **15**, 184 (1969).
32. Schuh, H., and B. Persson, *Intern. J. Heat Mass Transfer*, **7**, 1257 (1964).

Manuscript received November 20, 1969; revision received May 21, 1970; paper accepted May 25, 1970. Paper presented at AIChE Portland meeting.

Computation of Near-Optimal Control Policies by Trajectory Approximation: Hyperbolic-Distributed Parameter Systems with Space-Independent Controls

ELLIOT S. PARKIN and R. L. ZAHRADNIK

Carnegie-Mellon University, Pittsburgh, Pennsylvania

Trajectory approximations have been used to compute near-optimal control policies for a number of lumped-parameter systems. In this paper the technique is generalized to distributed-parameter systems. The essence of the method is the approximation of the state and adjoint variables of the problem by a linear combination of spatially dependent trial functions and time-dependent mixing coefficients. Application of the method of weighted residuals to the spatial variations reduces the problem to one involving a system of ordinary differential equations for the mixing coefficients.

Results are presented of an application of the algorithm to the determination of near-optimal control policies for a tubular plug-flow heat exchanger with uniform wall flux forcing. The results compare favorably with the optimal solutions and indicate that the method could be of considerable value in implementing optimal control for a wide class of systems.

The technique of using trajectory approximations to compute near-optimal control policies has been applied to a number of lumped-parameter systems (*8*, *10*). The method involves the approximation of the state and adjoint variables of an optimal control problem in terms of linear combinations of trial functions and mixing coefficients. The